Hindawi Publishing Corporation
Mathematical Problems in Engineering
Volume 2013, Article ID 257193, 8 pages
http://dx.doi.org/10.1155/2013/257193

Research Article

Design of the Microsatellite Attitude Control System Using the Mixed H_2/H_∞ Method via LMI Optimization

Erberson Rodrigues Pinheiro and Luiz Carlos Gadelha de Souza

Instituto Nacional de Pesquisas Espaciais (INPE), Avenida dos Astronautas 1758, 12227-101 So Jos Dos Campos, SP, Brazil

Correspondence should be addressed to Luiz Carlos Gadelha de Souza; gadelha@dem.inpe.br

Received 5 April 2013; Revised 4 July 2013; Accepted 11 July 2013

Academic Editor: Maria Zanardi

Due to the space missions limited budget, small satellite cluster or constellation would be an economical choice. From risk-sharing viewpoint, a number of smaller satellites have a significant reliability advantage over a bigger one. Generally, one satellite is subject to two types of uncertainties: structured uncertainty that represents some satellite parameter variation and the unstructured uncertainty that represents some kind of the satellite model error. On the other hand, the Satellite Attitude Control (SAC) design becomes more vulnerable to uncertainty disturbances like model error and moment-of-inertia variation as the satellite has great decrease in size and weight. This is the case for a microsatellite with mass less than 100 kg where the ACS performance and robustness become very sensitive to both kinds of uncertainties. As a result, the design of the SAC has to deal with both types of uncertainties which is associated with the drawback between controller performance and robustness. The purpose of this work is to model a microsatellite taking into account the uncertainties and to perform the Control System Design based on the mixed H_2/H_∞ methodology via LMI optimization.

1. Introduction

Microsatellites play an important role in space missions, such as position location, Earth observation, atmospheric data collection, space science, and communication. Some spacecrafts used to observation need high-accuracy performance on pointing requirement, so it is necessary to apply a three-axis attitude control, leading a multivariable control system [1]. In the face of disturbance and uncertainty, it is necessary to design a robust control for analysis and synthesis of attitude control system. Examples of satellite robust control system design using multiobjective and nonlinear approaches can be found in [2, 3], respectively. Low orbit spacecrafts are under a more strong influence of gravity gradient torque, aerodynamic torque, and magnetic torque. Some equipments on the microsatellite like cameras, telescopes, and solar array can move causing change on moment of inertia. Microsatellites with mass less than 100 kg are more sensitive to moment of inertia variation and disturbances like external torques [4].

In this work, we will be using a kind of robust control called mixed H_2/H_∞ control. This combination was introduced by Bernstein and Haddad [4]; where the idea was to minimize an H_2 norm of a transfer function subjected to a constraint given by a H_∞ norm of another transfer function. In the paper [5] was considered the state and the output feedback of the mixed H_2/H_∞ control to solve the non-linear Riccati equation in a convex optimization context. As for vibration control of rigid-flexible satellite, an alternative approach is to use piezoelectric shunt damping technique as has been done in [6]. In this work, one uses the mixed H_2/H_∞ control via the LMI approach [7] to design an attitude control of a microsatellite subjected to an external disturbances and with uncertainty in the moment of inertia.

2. Microsatellite Attitude Dynamics

It is defined as a body-fixed reference frame B with its origin located in the center of mass of a microsatellite and is given

the unit vectors $\{\mathbf{i},\mathbf{j},\mathbf{k}\}$ being along the principal axes. The Euler equations of a microsatellite are given by [7]

$$\begin{aligned} I_x\dot{\omega}_x - \left(I_y - I_z\right)\omega_y\omega_z &= T_{ex} + T_{gx} + u_x, \\ I_y\dot{\omega}_y - \left(I_z - I_x\right)\omega_z\omega_x &= T_{ey} + T_{gy} + u_z, \\ I_z\dot{\omega}_z - \left(I_x - I_y\right)\omega_x\omega_y &= T_{ez} + T_{gz} + u_z, \end{aligned} \tag{1}$$

where I_x, I_y, and I_z are the principal moments of inertia, ω_x, ω_y, and ω_z are the body-axis components of angular velocity, T_{ex}, T_{ey}, and T_{ez} are the nonmodelled external torques, T_{gx}, T_{gy}, and T_{gz} are the components of gravity gradient torques that will be inserted into the equations, and u_x, u_y, and u_z are the control torques.

It is necessary to consider another reference system A local-vertical local-horizontal (LVLH) with its origin at the center of mass of the microsatellite. The LVLH frame has the following unitary vectors $\{\mathbf{a_1},\mathbf{a_2},\mathbf{a_3}\}$, with $\mathbf{a_1}$ in the direction of the microsatellite velocity in the orbital plane, $\mathbf{a_3}$ pointing to the Earth, and $\mathbf{a_2}$ normal to the orbit plane.

To describe the orientation of the body-fixed frame B with respect of LVLH frame in terms of Euler angles, the following coordinate transformation is used:

$$\begin{bmatrix} \mathbf{i} \\ \mathbf{j} \\ \mathbf{k} \end{bmatrix} = \begin{bmatrix} c\theta c\psi & c\theta s\psi & -s\theta \\ s\phi s\theta c\psi - c\phi s\psi & s\phi s\theta s\psi + c\phi c\psi & s\phi c\theta \\ c\phi s\theta c\psi + s\phi s\psi & c\phi s\theta s\psi - s\phi c\psi & c\phi c\theta \end{bmatrix} \begin{bmatrix} \mathbf{a_1} \\ \mathbf{a_2} \\ \mathbf{a_3} \end{bmatrix}. \tag{2}$$

The angular velocity of the body-fixed frame B relative to the LVLH is given by

$$\begin{aligned} \vec{\omega}^{B/A} &= \omega_x^{B/A}\mathbf{i} + \omega_y^{B/A}\mathbf{j} + \omega_z^{B/A}\mathbf{k}, \\ \begin{bmatrix} \omega_x^{B/A} \\ \omega_y^{B/A} \\ \omega_z^{B/A} \end{bmatrix} &= \begin{bmatrix} 1 & 0 & -s\theta \\ 0 & c\phi & s\phi c\theta \\ 0 & -s\phi & c\phi c\theta \end{bmatrix} \begin{bmatrix} \dot{\phi} \\ \dot{\theta} \\ \dot{\psi} \end{bmatrix}. \end{aligned} \tag{3}$$

The angular velocity of the body fixed frame B relative to the inertial frame N fixed in the Earth center becomes

$$\vec{\omega} = \vec{\omega}^{B/N} = \vec{\omega}^{B/A} + \vec{\omega}^{A/N} = \vec{\omega}^{B/A} - n\vec{a}_2, \tag{4}$$

where

$$\begin{bmatrix} \omega_x \\ \omega_y \\ \omega_z \end{bmatrix} = \begin{bmatrix} 1 & 0 & -s\theta \\ 0 & c\phi & s\phi c\theta \\ 0 & -s\phi & c\phi c\theta \end{bmatrix} \begin{bmatrix} \dot{\phi} \\ \dot{\theta} \\ \dot{\psi} \end{bmatrix} - n \begin{bmatrix} c\theta s\psi \\ s\phi s\theta s\psi + c\phi c\psi \\ c\phi s\theta s\psi - s\phi c\psi \end{bmatrix}. \tag{5}$$

n is the orbital frequency of the microsatellite.

For small attitude deviation from LVLH orientation, the following linearized attitude dynamics can be obtained as follows:

$$\begin{aligned} \omega_x &= \dot{\phi} - n\psi, \\ \omega_y &= \dot{\theta} - n, \\ \omega_z &= \dot{\psi} + n\phi. \end{aligned} \tag{6}$$

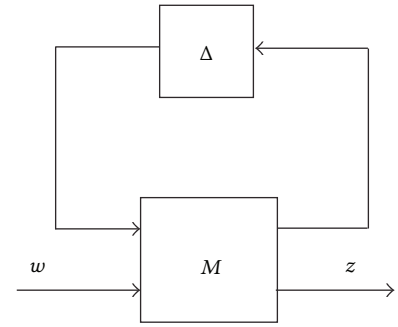

Figure 1: Uncertainty representation in LFT block diagram.

2.1. Gravity Gradient Torque. In the space, the gravitational field is not uniform, so the variation in the gravitational field over the body yields the gravitational torque of the center of mass of the body. On the assumption that the microsatellite center of mass is in a Keplerian circular orbit and the Earth is spherical, the gravity gradient torque along the body axes becomes [8]

$$\begin{aligned} T_{gx} &= 3n^2\left(I_z - I_y\right)\phi, \\ T_{gy} &= 3n^2\left(I_z - I_x\right)\theta, \\ T_{gz} &= 0. \end{aligned} \tag{7}$$

Inserting the gravity gradient equations (7) into the Euler equations (1) and making a linearization, one has

$$\begin{aligned} u_x + T_{d_x} &= I_x\ddot{\phi} - n\left(I_x - I_y + I_z\right)\dot{\psi} + 4n^2\left(I_y - I_z\right)\phi, \\ u_y + T_{d_y} &= I_y\ddot{\theta} + 3n^2\left(I_x - I_z\right)\theta, \\ u_z + T_{d_z} &= I_z\ddot{\psi} + n\left(I_x - I_y + I_z\right)\dot{\phi} + n^2\left(I_y - I_x\right)\psi. \end{aligned} \tag{8}$$

These equations are the Euler equations for the microsatellite, from which one observes that the pitch axis is decoupled from the row and yaw axes.

3. Structured Uncertainty

To represent the system uncertainty Δ it will be used Linear Fractional Transformation (LFT) [9]. As shown in Figure 1, using the LFT procedure the block transfer function from the perturbation signal w to error signal z is given by

$$z = \left[M_{22} + M_{21}\Delta\left(I - M_{11}\Delta\right)^{-1}M_{12}\right]w. \tag{9}$$

The plant of the system can be represented by the block M which is given by

$$M = \begin{bmatrix} M_{11} & M_{12} \\ M_{21} & M_{22} \end{bmatrix}. \tag{10}$$

Considering that there is uncertainty in the principal moment of inertia of the microsatellite, it can be expressed as a nominal value plus a perturbation [7] given by

$$I_i = \bar{I}_i + p_i\delta_i, \quad \left|\delta_i\right| \le 1, \ i = x, y, z, \tag{11}$$

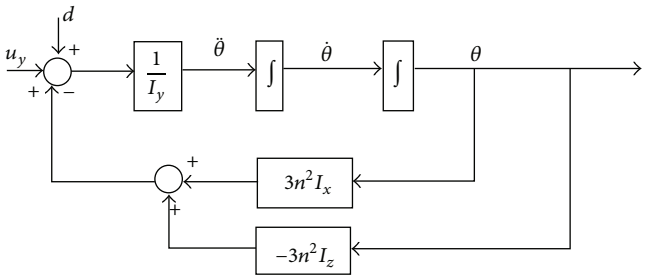

Figure 2: Block diagram of the pitch axis.

where p_i is the variation and δ_i is the normalized uncertainty. Inserting it into the Euler equations, one has the dynamic equation with uncertainty. This uncertainty can be pulled out of the system, and it can be considered as a disturbance.

Let us do this calculation, initially, for pitch axis of the microsatellite which is decouple, d is the disturbing torque. As result, the equation of motion is given by

$$I_y\ddot{\theta} + 3n^2\left(I_x - I_z\right)\theta = u_y + d. \tag{12}$$

This equation of motion can be put in the block diagram as shown in Figure 2.

Using the Linear Fractional Transformation (LFT), the first block of the Figure 2 can be represented by

$$\begin{aligned}\frac{1}{I_y} &= \frac{1}{\overline{I}_y + p_y\delta_y},\\ &= \frac{1}{\overline{I}_y} - \frac{p_y}{\overline{I}_y}\delta_y\left(1 + \frac{1}{\overline{I}_y}\delta_y\right)^{-1}\frac{1}{\overline{I}_y}.\end{aligned} \tag{13}$$

Comparing this equation with the LFT (9), the first block will be

$$M_1 = \begin{bmatrix} -\dfrac{p_y}{\overline{I}_y} & \dfrac{1}{\overline{I}_y} \\ -\dfrac{p_y}{\overline{I}_y} & \dfrac{1}{\overline{I}_y} \end{bmatrix}. \tag{14}$$

Doing the same procedure for the second and the third block is given by

$$\begin{aligned} 3n^2I_x &= 3n^2\left(\overline{I}_x + p_x\delta_x\right),\\ M_2 &= \begin{bmatrix} 0 & 1 \\ 3n^2p_x & 3n^2\overline{I}_x \end{bmatrix},\\ 3n^2I_z &= 3n^2\left(\overline{I}_z + p_x\delta_z\right),\\ M_3 &= \begin{bmatrix} 0 & -1 \\ 3n^2p_z & -3n^2\overline{I}_z \end{bmatrix}. \end{aligned} \tag{15}$$

As a result, the new block diagram for the pitch axis taking into account the uncertainty is as shown in Figure 3.

This representation helps to understand how the uncertainty acts in the system and how it can be lumped out of the system like a perturbation. Usually, the uncertainty is incorporated in the generalized plant in the diagonal form as shown in Figure 4.

The generalized plant P represented in Figure 4 can be given by

$$P = \begin{bmatrix} A & B_1 & B_2, \\ C_1 & D_{11} & D_{12}, \\ C_2 & D_{21} & D_{22} \end{bmatrix}. \tag{16}$$

Taking into account all derivations performed up to now and the relationship between the input and the output of the microsatellite system, one obtains the generalized plant in matrix form given by

$$\begin{bmatrix} \dot{\theta} \\ \ddot{\theta} \\ y_1 \\ y_2 \\ y_3 \\ y \end{bmatrix} = \begin{bmatrix} 0 & 1 & 0 & 0 & 0 & 0 & 0 \\ \dfrac{-3n^2\left(I_x - I_z\right)}{I_y} & 0 & -\dfrac{p_y}{I_y} & -\dfrac{3n^2p_x}{I_y} & -\dfrac{3n^2p_z}{I_y} & -\dfrac{1}{I_y} & -\dfrac{1}{I_y} \\ \dfrac{-3n^2\left(I_x - I_z\right)}{I_y} & 0 & -\dfrac{p_y}{I_y} & -\dfrac{3n^2p_x}{I_y} & -\dfrac{3n^2p_z}{I_y} & -\dfrac{1}{I_y} & -\dfrac{1}{I_y} \\ 1 & 0 & 0 & 0 & 0 & 0 & 0 \\ -1 & 0 & 0 & 0 & 0 & 0 & 0 \\ 1 & 0 & 0 & 0 & 0 & 0 & 0 \\ 1 & 0 & 0 & 0 & 0 & 0 & 0 \end{bmatrix} \times \begin{bmatrix} \theta \\ \dot{\theta} \\ u_1 \\ u_2 \\ u_3 \\ d \\ u \end{bmatrix}. \tag{17}$$

The mixed design H_2/H_∞ aprroach consists first to minimizing the perturbation effect of moment of inertia uncertainty (structured) by the H_∞ norm. The closed loop system will be robust and stable for any uncertainty satisfying the relation $\|\Delta\|_\infty < 1/\gamma$. Specifically the lower the value of γ; the closed loop system remains stable for a large uncertainty, that is, a large range of inertia moment variation.

On the other hand, the external disturbance uncertainty (unstructured) will be minimized by the H_2 norm. As a result, the closed loop system remains stable for external perturbation, which is associated with good performance, for example, quick time response and small overshot.

Therefore, in order to include both kinds of uncertainties so as the controller designed presents good robustness and adequate performance, the new generalized plant must have

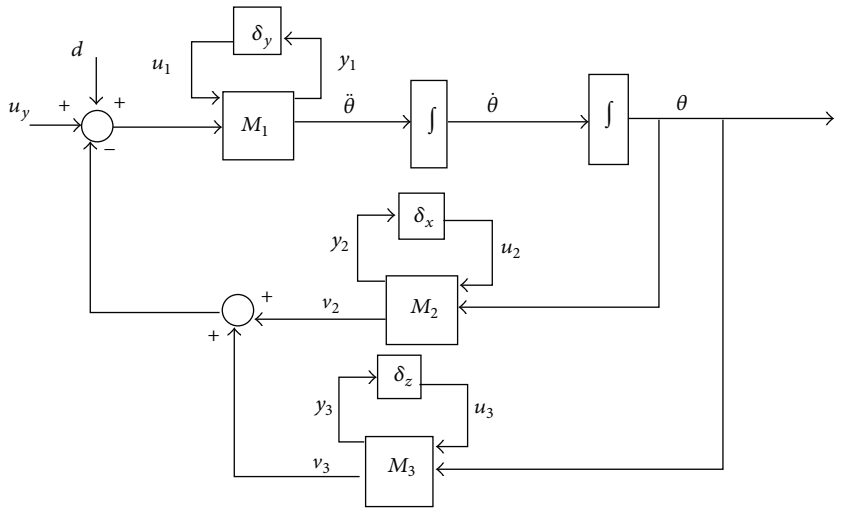

Figure 3: The block diagram for the pitch axis with uncertainty.

both signals that will be minimized. Here, the generalized plant in matrix form is given by

$$\begin{bmatrix} \dot{\theta} \\ \ddot{\theta} \\ z_\infty \\ z_2 \\ y \end{bmatrix} = \begin{bmatrix} 0 & 1 & 0 & 0 & 0 & 0 & 0 \\ \frac{-3n^2(I_x - I_z)}{I_y} & 0 & -\frac{p_y}{I_y} & -\frac{3n^2 p_x}{I_y} & -\frac{3n^2 p_z}{I_y} & -\frac{1}{I_y} & -\frac{1}{I_y} \\ \frac{-3n^2(I_x - I_z)}{I_y} & 0 & -\frac{p_y}{I_y} & -\frac{3n^2 p_x}{I_y} & -\frac{3n^2 p_z}{I_y} & -\frac{1}{I_y} & -\frac{1}{I_y} \\ 1 & 0 & 0 & 0 & 0 & 0 & 0 \\ -1 & 0 & 0 & 0 & 0 & 0 & 0 \\ Q_1 & 0 & 0 & 0 & 0 & 0 & 0 \\ 0 & Q_2 & 0 & 0 & 0 & 0 & 0 \\ 0 & 0 & 0 & 0 & 0 & 0 & R \\ 1 & 0 & 0 & 0 & 0 & 0 & 0 \end{bmatrix} \times \begin{bmatrix} \theta \\ \dot{\theta} \\ u_1 \\ u_2 \\ u_3 \\ d \\ u \end{bmatrix}. \tag{18}$$

In that case, one has the inputs (u_1, u_2, u_3, u), the outputs (z_∞, z_2, y), the states $(\theta, d\theta/dt)$, and the perturbation $d = w$.

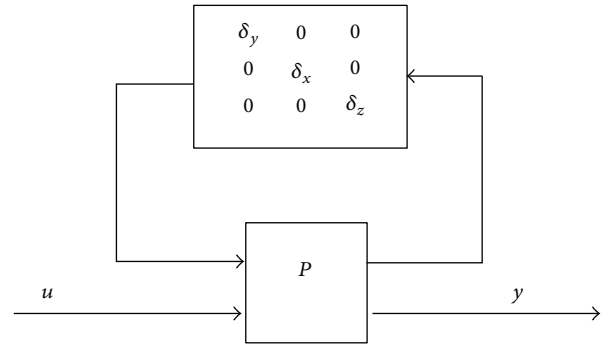

Figure 4: Generalized plant with uncertainty organized in the diagonal form.

As a result, the new state space model that includes both kinds of design requirements is given by

$$\begin{aligned} \dot{x} &= Ax + B_1 w + B_2 u, \\ z_\infty &= C_1 x + D_{11} w + D_{12} u, \\ z_2 &= C_2 x + D_{22} u. \end{aligned} \tag{19}$$

4. The Mixed H_2/H_∞ Controller Theory

Figure 5 shows the block diagram of the mixed H_2/H_∞ control approach [5], where the above block represents the uncertainty; the medium block is the generalized plant, and the below block is the controller to designed.

The mixed H_2/H_∞ controller design is a multiobjective control problem where the goal is to minimize the H_2 norm in order to improve performance subjected to the minimization of H_∞ norm to guaranty robustness requirement [9] which can be expressed by

$$\begin{aligned} &\text{minimize} \qquad f(K) := \left\| T_{wz_2} \right\|_2^2 \\ &\text{subjected to} \quad g(K) := \left\| T_{wz_\infty} \right\|_\infty^2 \le \gamma^2. \end{aligned} \tag{20}$$

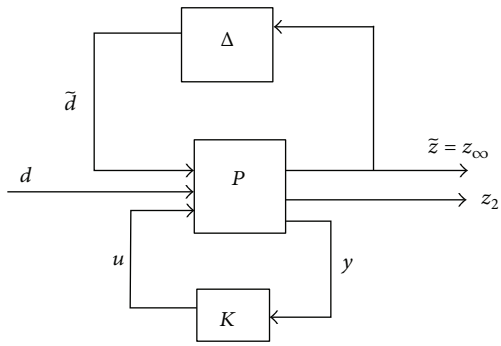

Figure 5: The general configuration of mixed H_2/H_∞ control design.

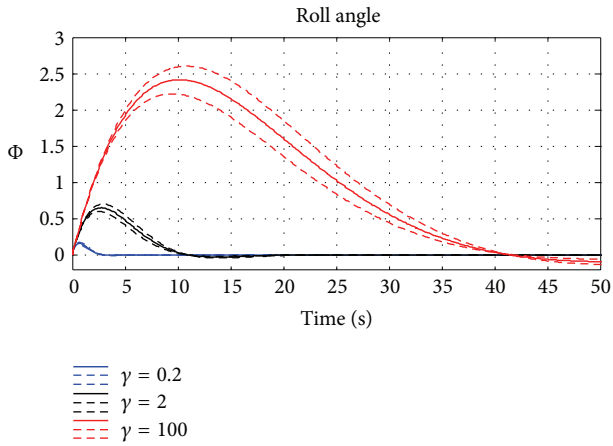

Figure 6: The mixed H_2/H_∞ controller for Euler angle of roll with uncertainty.

As shown in [8], the mixed H_2/H_∞ control problem is equivalent to minimizing Trace Tr(Q) over the matrices $X = X^T$, $Q = Q^T$, and Y satisfying the Linear Matrix Inequalities [9] given by

$$\begin{bmatrix} AX - B_2Y + (AX - B_2Y)^T & B_1 & (C_\infty X - D_{\infty 2}Y)^T \\ B_1^T & -I & D_{\infty 1}^T \\ C_\infty X - D_{\infty 2}Y & D_{\infty 1} & \gamma^2 I \end{bmatrix} < 0,$$

$$\begin{bmatrix} Q & C_2X - D_{22}Y \\ (C_2X - D_{22}Y)^T & X \end{bmatrix} > 0. \tag{21}$$

Assuming that the LMIs (22) and (23) have solutions Y^*, X^*, and Q^*, the mixed H_2/H_∞ controller K^* is given by

$$K^* = Y^*(X^*)^{-1}, \tag{22}$$

which results in the following two expressions:

$$\| T_{wz_\infty} \|_\infty \le \gamma,$$
$$\| T_{wz_2} \|_2 \le \sqrt{\mathrm{Tr}\,(Q)}. \tag{23}$$

Table 1: Star sensor data.

Properties	Value
Size	$10 \times 10 \times 4.5$ cm
Mass	10 gr
Accuracy	1 arcseg
Angular velocity	above 10°/s
Reliability	99.99%
Rate of actualization	8 Hz

Table 2: Actuator: reaction wheel.

Speed range (rpm)	±10000
Momentum capacity (N m s)	4
Reaction torque (N m)	150×10^{-3}
Mass (Kg)	
Reaction wheel	<3.55
Motor driver	<1.2
Dimension (cm)	$25 \times 25 \times 11$

5. Simulations and Results

The information about the microsatellite used in the simulation is given by Tables 1 and 2.

In the mixed H_2/H_∞ controller design, a key point is to find the appropriate values of γ. Besides, one must keep in mind that for $\gamma = \gamma_{\min}$ one has the pure H_∞ control problem, and for $\gamma = \gamma_{\max}$ one has the pure H_2 control problem. Here, just for simulations propose one decides to begin using $\gamma = 2$ to perform a comparative study. As for the uncertainty, one assumes that the variation on the moment of inertia is about 10%. In order to obtain the maximum and the minimum uncertainty variations, one considers two kinds of plants given by

(i) Variation in the inertia moment for pitch angle:

Plant with uncertainty 1: $\Delta I_x = -10\% I_x$, $\Delta I_y = +10\% I_y$ and $\Delta I_z = -10\% I_z$.

Plant with uncertainty 2: $\Delta I_x = +10\% I_x$, $\Delta I_y = -10\% I_y$ and $\Delta I_z = +10\% I_z$.

(ii) Variation in the inertia moment for pitch angle for roll and yaw angles:

Plant with uncertainty 1: $\Delta I_x = +10\% I_x$, $\Delta I_y = -10\% I_y$ and $\Delta I_z = -10\% I_z$.

Plant with uncertainty 2: $\Delta I_x = -10\% I_x$, $\Delta I_y = +10\% I_y$ and $\Delta I_z = +10\% I_z$.

(iii) Initial conditions:

$$x(0) = [0 \;\; 0 \;\; 0],$$
$$\dot{x}(0) = [0,6 \;\; 0,6 \;\; 0,6]. \tag{24}$$

In Figures 6, 7, and 8 the dashed line represents the plant with uncertainty variation, and the continues line represents the nominal plant without uncertainty. They show the Euler angles (roll, pitch, and yaw) control for pure H_∞ control ($\gamma =$

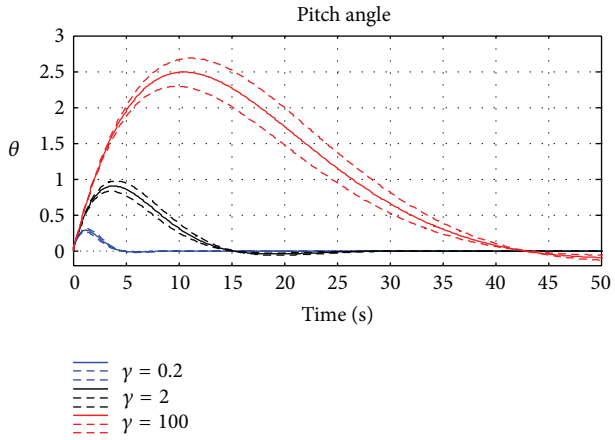

Figure 7: The mixed H_2/H_∞ controller for Euler angle of pitch with uncertainty.

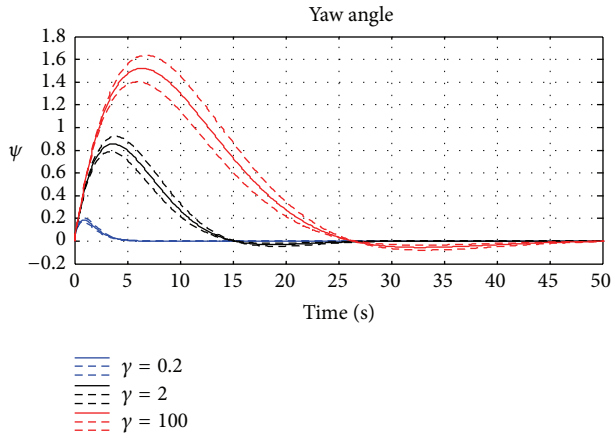

Figure 8: The mixed H_2/H_∞ controller for Euler angle of pitch with uncertainty.

$\gamma_{\min} = 0.2$-blue line); the controller is very robust with respect to uncertainty, because there is no difference between the nominal plant and the plant with uncertainty. On the other hand, it is noted that the difference between the nominal plant and the plant with uncertainty increases for pure H_2 control ($\gamma = \gamma_{\max} = 100$-red line).

Figures 9, 10, and 11 show that for pure H_∞ control (blue line), the controller signal has bigger overshot than for pure H_2 control (red line), which represents the drawback between its robustness and performance. Considering that the microsatellite actuator must have small torque, the mixed H_2/H_∞ control with $\gamma = 2$ is a good choice to design the controller, because it is not so slow like pure H_2, and the control signal is not so strong like pure H_∞ control.

Spacecraft is subjected to small disturbances on the space, and these disturbances can be persistent. In the case of a low orbit, the microsatellite is more subject to disturbances due to the gravity gradient, magnetic, and aerodynamic torques. The gravity gradient torque is included into the equations, the magnetic torque is cyclic and can be approximated by sinusoids with different frequencies, and the aerodynamic

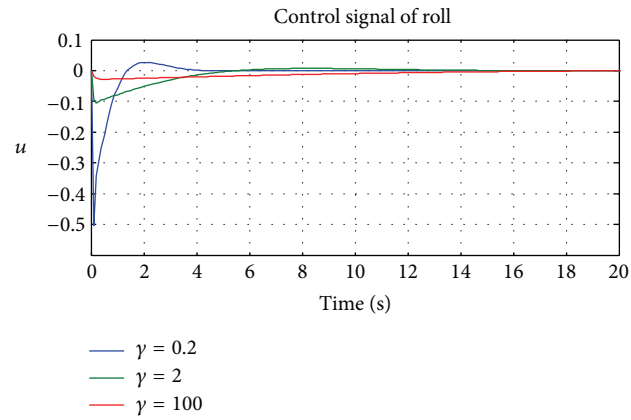

Figure 9: The mixed H_2/H_∞ controller signal for the roll axis.

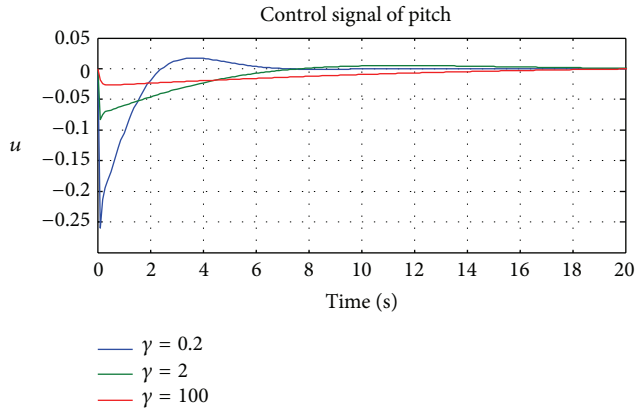

Figure 10: The mixed H_2/H_∞ controller signal for the pitch axis.

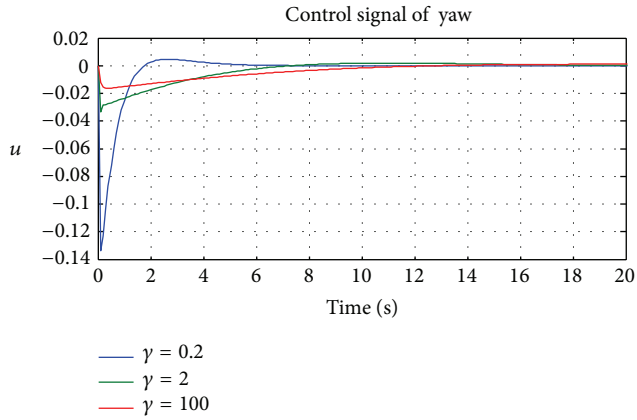

Figure 11: The mixed H_2/H_∞ controller signal for the yaw axis.

torque is cumulative and can be approximated to a step. As a result, one has assumed that these torques can be represented by the following equation:

$$T_{\text{ext}} = \sum_k 10^{-5} \text{sen}\,(knt) + 3 \times 10^{-5} \left[\sigma\,(t - 1000) - \sigma\,(t - 4000)\right]. \quad (25)$$

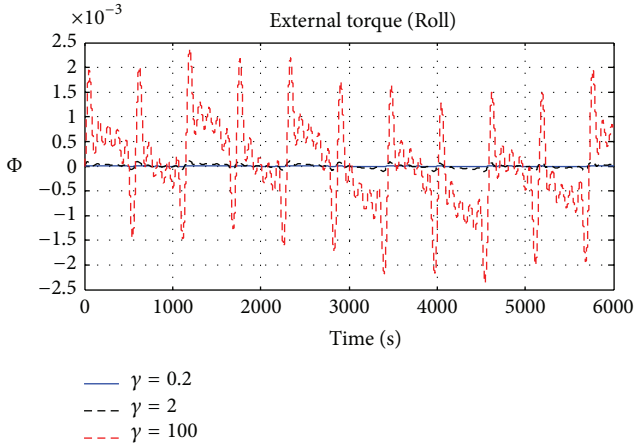

FIGURE 12: The mixed H_2/H_∞ controller response to external torques for the roll axis.

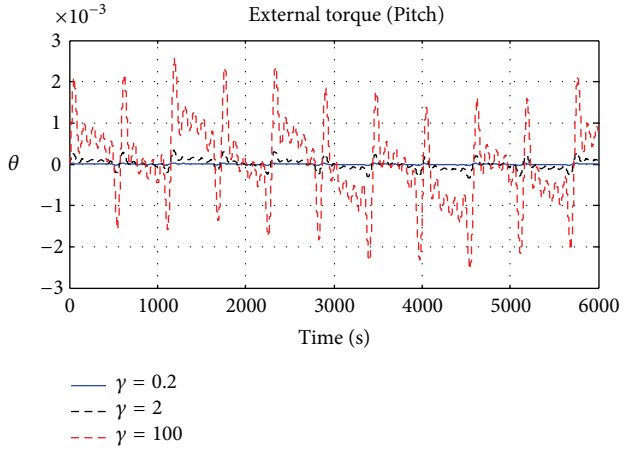

FIGURE 13: The mixed H_2/H_∞ controller response to external torques for the pitch axis.

Figures 12, 13, and 14 show the Euler angles (roll, pitch, yaw) for the pure H_∞ control (blue line), the mixed control H_2/H_∞ (γ = 2-black line), and the pure H_2 control (red line). One observes that the pure H_∞ control has the best capacity of attenuation with respect to a sinusoidal disturbance. The pure H_2 control is not robust with respect to a sinusoidal disturbance. In order to have a good balance control between robustness and performance one must choose some values of γ such that the mixed control H_2/H_∞ provide a good performance even with the perturbation of the external torques. Again, the best mixed control H_2/H_∞ controller value for γ is 2.

6. Conclusion

This paper presents a microsatellite model taking into account the uncertainties and the design of the satellite control system based on the mixed H_2/H_∞ methodology via LMI optimization. This control technique is used to design the microsatellite attitude control system in the face of

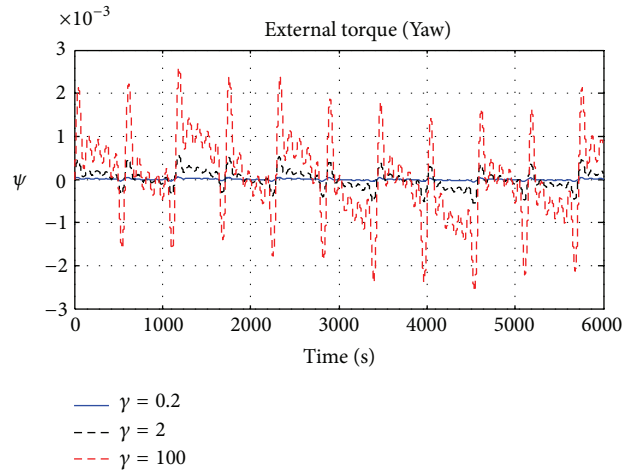

FIGURE 14: The mixed H_2/H_∞ controller response to external torques for the yaw axis.

environmental disturbance (unstructured uncertainty) and moment of inertia variation (structured uncertainty). It is well know that the H_∞ controller provides robust stability with respect to structured uncertainty while the H_2 controller provides good performance with respect to unstructured uncertainty. Here, one investigates the conjunction of both methods in order to improve the performance and robustness of the SAC system. To do this, one assumes that the microsatellite is subjected to uncertainty in the moment of inertia variation of about 10%, and environmental disturbances were approximated to sinusoidal function plus a step function. The simulations have shown that the H_∞ controller has presented the best robustness and performance than the H_2 controller with respect to uncertainty due to inertia moment variation and due to external disturbance. However, in all simulations the H_∞ controller signal was bigger than the H_2 controller, which can cause bigger overshot and can saturate the actuator, once the microsatellite usually needs a small actuator. As a result, the way to achieve robustness stability and good performance was to design the controller using the mixed H_2/H_∞ control, because in this procedure one can choose an adequate value for the tuning parameter γ so as one can have robust control and with low control signal.

References

[1] X. C. Méndez Cubillos and L. C. G. de Souza, "Using of H-infinity control method in attitude control system of rigid-flexible satellite," *Mathematical Problems in Engineering*, vol. 2009, Article ID 173145, 9 pages, 2009.

[2] I. Mainenti, L. C. G. Souza, and F. L. Souza, "Design of a nonlinear controller for a rigid-flexible satellite using multi-objective generalized extremal optimization with real codification," *Shock and Vibration*, vol. 19, pp. 1–10, 2012.

[3] L. C. G. Souza and R. G. Gonzalez, "Application of the state-dependent riccati equation and kalman filter techniques to the design of a satellite control system," *Shock and Vibration*, vol. 19, pp. 22–28, 2012.

[4] D. S. Bernstein and W. M. Haddad, "LQG control with an H_∞ performance bound: a Riccati equation approach," *IEEE Transactions on Automatic Control*, vol. 34, no. 3, pp. 293–305, 1989.

[5] P. P. Khargonekar and M. A. Rotea, "Mixed H_2/H_∞ control: a convex optimization approach," *IEEE Transactions on Automatic Control*, vol. 36, no. 7, pp. 824–837, 1991.

[6] T. P. Sales, D. A. Rade, and L. C. G. Souza, "Passive vibration control of flexible spacecraft using shunted piezoelectric transducers," *Aerospace Science and Technology*, vol. 1, pp. 12–26, 2013.

[7] C.-D. Yang and Y.-P. Sun, "Mixed H_2/H_∞ state-feedback design for microsatellite attitude control," *Control Engineering Practice*, vol. 10, no. 9, pp. 951–970, 2002.

[8] J. R. Wertz and W. J. Larson, *Space Mission Analysis and Design*, Microcosm Press, Hawthorne, Calif, USA, 1989.

[9] S. Boyd, L. El Ghaoui, E. Feron, and V. Balakrishnan, *Linear Matrix Inequalities in System and Control Theory*, SIAM Studies in Applied Mathematics, SIAM, Philadelphia, Pa, USA, 1994.